*Scientific Journal of the Ternopil National Technical University*
*2026, vol. 122, no. 2, pp. 120–129,*
*ISSN: 2522-4433 Print, ISSN: 2522-4441 Online*
*https://doi.org/10.35784/ visnyk_tntu2026.02.120*

*Submitted: 2026-02-02 | Revised: 2026-03-17 | Accepted: 2026-05-26*



# Comparison of tribological properties of VT6 titanium alloy surface after oxidation and nitriding

**Mykhailo Student[1],*, Alexander Luk'yanenko[1], Iryna Pohrelyuk[1], Khrystyna Zadorozhna[1], Oleksandra Student[1], Vasyl Trush[1], Volodymyr Hvozdetskyi[1]**

[1]Karpenko Physico-Mechanical Institute of the National Academy of Sciences of Ukraine, Lviv, Ukraine, e-mail pminasu@ipm.lviv.ua

* Corresponding author student.phmi@gmail.com

**Abstract:** *Titanium alloys offer advantages over steel due to their low specific density and high specific strength. This makes them indispensable in products for the aerospace, marine, and damping industries, among others. However, their poor frictional properties significantly limit their applications. This study proposes a way to minimize this disadvantage of titanium alloys by modifying their surface layers using an advanced thermochemical treatment (TCT) in a gas environment with controlled oxygen and nitrogen contents. Surface layers of VT6 titanium alloy were modified at 750°C with limited oxygen access and a controlled nitrogen flow. This TCT mode limited the thickness of TiO2 or TiN uniform layers formed on the surface of the alloy to 1–2 μm. Immediately beneath them, layers of solid-solution-hardened material with a gradient of oxygen or nitrogen content formed. Their microhardness gradually decreased, reaching the level of untreated titanium at a depth of 29–30 μm. To confirm the effectiveness of TCT, a friction test method was used under conditions of oscillatory sliding of steel and ceramic balls (as counterbodies) on a hardened surface. Wear profiles revealed small indentations from spherical counterbodies into the surface-hardened layers (from 3 to 1 μm under dry friction and boundary lubrication conditions, respectively). Hard particles of titanium dioxide or nitride altered the wear track profile on the surface of the TCT samples from relatively uniform to textured due to the selective removal of small chips. Despite the higher microhardness, the nitrided layer turned out to be 40-50% worse than the oxidized layer in terms of wear resistance, and this did not depend on the friction conditions (counterbody material, friction conditions, or the type of lubricant used). This was explained by the charging of the surface layers of the samples with superhard TiN fragments that entered the friction zone. Under dry friction, the friction coefficient between the steel ball and the surface-hardened VT6 alloy remained stable, but increased when using a ceramic ball. Under boundary lubrication, the friction coefficient remained constant by removing wear debris from the friction zone. Overall, the tests showed that controlled surface oxidation of the VT6 titanium alloy provides superior wear resistance compared to nitriding.*

**Keywords:** *VT6 titanium alloy, thermochemical treatment; solid-solution hardening; microhardness; oscillatory sliding friction; boundary lubrication; wear resistance; friction coefficient.*

## 1. INTRODUCTION

The unique synergy of low density, high specific strength, and excellent corrosion resistance renders titanium alloys indispensable for critical industrial applications, particularly in the aerospace, maritime, and defense sectors [1–3]. Furthermore, nickel-titanium (nitinol) alloys – characterized by exceptional super elasticity and shape memory effects – are vital for fabricating structural dampers used in seismic mitigation [4–6]. Within the aerospace industry, which currently consumes half of the global titanium supply, these alloys are utilized for compressor disks and blades, air intake components, guide vanes, and fasteners [7]. This consumption is projected to double over the next decade.

Beyond mechanical strength, titanium’s low coefficient of thermal expansion ensures the dimensional stability of structural components, such as hydraulic engine cylinders. This stability is critical for both high-precision military hardware and specialized civilian applications, including agricultural herbicide spraying systems. Notably, titanium alloys remain unrivaled for aircraft engines operating at Mach 2.0 to 3.5.

Despite these advantages, the replacement of steel fasteners with titanium alternatives is hindered by titanium’s inherent susceptibility to galling (seizure) [7]. Technical data indicates that when titanium alloys interface with harder metals, titanium tends to transfer (adhere) to the counter-body surface, resulting in titanium-on-titanium friction. Conversely, when in contact with softer metals, the softer material transfers to the titanium surface. This adhesive wear complicates disassembly during maintenance and repair. To mitigate this, wear-resistant anti-seizure layers are typically engineered onto the fastener surfaces [8–11].

The widespread implementation of titanium alloys is further restricted by their poor tribological properties. Due to titanium's high chemical affinity for oxygen, it naturally forms a thin, stable oxide film that exhibits poor wettability with mineral oils, leading to a high coefficient of friction during sliding. Thermochemical treatment (TCT) technologies, specifically diffusion coating, offer a robust solution to improve these tribological characteristics. Interstitial strengthening of surface layers with oxygen or nitrogen – followed by the formation of discrete oxide or nitride surface films – retains the original dimensions of the components, a significant advantage for manufacturing precision [12–15].

The performance of these strengthened layers is heavily influenced by the magnitude and sign of residual stresses [16]. These stresses emerge during the cooling phase of TCT due to elastic interactions and mismatches in specific volume and the coefficient of thermal expansion (CTE) between the diffusion layer and the substrate. To optimize the balance of strength and toughness, TCT is often integrated with heat treatment, allowing for the simultaneous batch processing of numerous components [17, 18].

However, a lack of comprehensive data regarding the tribological behavior of surface-hardened titanium alloys by TCT limited their industrial adoption.

This study aims to develop of diffusion-modified layers by interstitials elements on the VT6 titanium alloy and demonstrate the efficacy of TCT (specifically oxidation and nitriding) as an excellent method for enhancing tribological performance.

## 2. METHODS

The tribological properties were investigated using the two-phase VT6 titanium alloy. The alloy microstructure primarily consists of an aluminum-stabilized α-phase (hexagonal close-packed lattice) and a secondary vanadium-stabilized β-phase (body-centered cubic lattice). The chemical composition of the alloy, compliant with GOST 19807-91, is as follows (wt.%): 6.2 Al, 4.3 V, 0.3 Fe, 0.1 C, 0.1 Si, 0.2 O, 0.05 N, and 0.015 H.

Surface hardening was performed using an enhanced thermochemical treatment (TCT) technology [19]. Specimens were prepared as plates ($15 \times 25 \times 1$ mm) with plane-parallel polished surfaces. The TCT process was conducted in an electric vacuum furnace at 750°C for 2–5 hours under a controlled atmosphere (oxygen or nitrogen content).

The phase composition of the solid-solution-hardened surface layers was characterized by X-ray diffraction (XRD) using a DRON-3.0 diffractometer with monochromatic CuKα radiation in a Bragg–Brentano geometry. Scanning was performed with a step size of 0.05°. Diffraction maxima and phase lattice parameters were determined using Sietronix, PowderCell 2.4, and FullProf software, with reference data from the JCPDS-ASTM databases.

The structural features of the diffusion-saturated layers and the resulting wear mechanisms were analyzed via scanning electron microscopy (SEM) using an EVO 40XVP system. Elemental mapping and composition of the structural components were performed using an INCA Energy 350 energy-dispersive X-ray spectroscopy (EDS) system.

Tribological performance was evaluated using reciprocating friction tests. The counterfaces consisted of steel (ShKh15/AISI 52100, 62 HRC) or ceramic ($Al_2O_3$ ) balls with a diameter of 10 mm (Fig. 1 a). Tests were conducted under dry friction and boundary lubrication conditions using two types of lubricants: mineral oil (I-20) and synthetic oil (EDGE 5W-30). The applied load was 10 N, and the total sliding distance was 1600 mm for all tests. Wear was quantified by averaging five cross-sectional area measurements taken at different points along the wear track. Wear track profiles were recorded using a «Caliber S-265» profilometer-profilograph (Fig. 1 b).

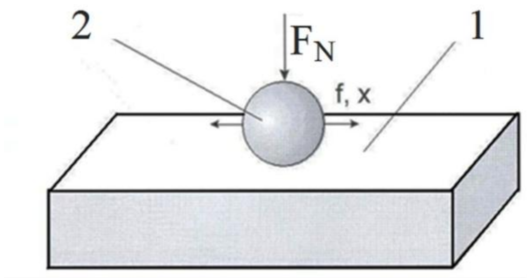


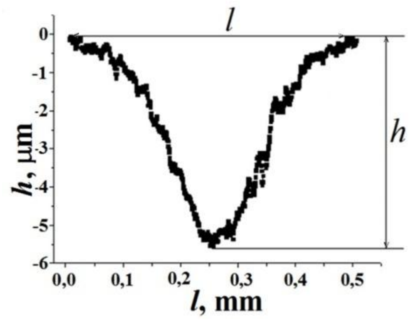


**(a)** **(b)**

**Figure 1.** Schematic representation of the friction tests: (a) oscillatory sliding of a counterbody made of a steel or ceramic ball on the surface of hardened VT6 alloy and (b) typical cross-sectional geometry of a wear track of depth h and width l. 1 – polished specimen surface; 2 – counterbody (ball rigidly fixed to the loading beam); FN – applied normal force.

The cross-sectional area of the wear track (S) in any given section was calculated using the following expression:

$$S = \sum_{i=0}^{l} \left| h(x_i) \right| \Delta x_i ,$$

where: h – is the wear groove depth on the hardened layer surface, determined from the cross-sectional profile (µm); l – is the width of the groove (mm); h(xi) – is the groove depth at each i-th point of the scanned section (µm); Δxi – is the sampling interval along the width of the wear track section where hi and li were measured. The microhardness of the modified layers was measured using a PMT-3M tester under a constant load of 0.49 N (50 gf).

## 3. RESULTS AND DISCASSION

### 3.1. Structural and Phase Analysis of Modified Surface Layers

Structural and phase analysis of the VT6 alloy surface layers after TCT revealed no morphological evidence of distinct bulk phases within the immediate subsurface region. This indicates that the hardening mechanism is mainly due to solid solution strengthening. (Fig. 2). X-ray diffraction (XRD) analysis identified a thin phase layer close to titanium dioxide (~TiO2) on the surface of the oxygen-modified specimens. In contrast, the nitrogen-modified specimens exhibited a titanium nitride phase with a stoichiometric composition of approximately ~TiN1.83 (Fig. 3). However, the thickness of these compound layers (oxide or nitride) did not exceed 2 μm. In contrast, the diffusion zones strengthened by the solid solution of oxygen or nitrogen reached significantly greater depths, ranging from 50 to 100 μm.

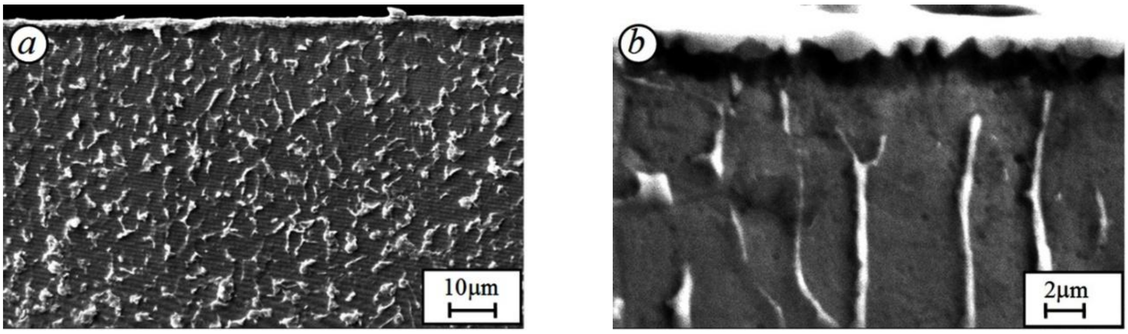


(a) (b)

**Figure 2.** Cross-sectional microstructure of the diffusion-modified layers on the VT6 titanium alloy after (a) oxidation and (b) nitriding.

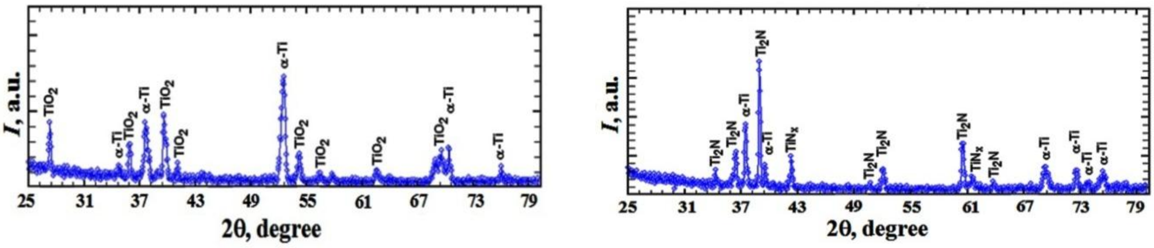


(a) (b)

**Figure 3.** X-ray diffraction patterns of surface layers of the VT6 alloy after diffusion solid solution strengthening with oxygen (a) and nitrogen (b). Opposite the reflections on the diffraction patterns, the corresponding phases are indicated.

According to the results of micro-X-ray spectral analysis of the content of elements in the oxidized layer on the surface of the VT6 alloy (by scanning over the area), 14.28 wt.% oxygen was found in its composition (Table 1), which confirmed the implementation of solid solution hardening. The same studies of the nitrided surface layer on the VT6 alloy revealed not only nitrogen (9.45 wt.%), but also a fairly significant amount of oxygen (4.28 wt.%, Table 1). The appearance of oxygen in the spectrum of the nitrided layer was explained by the use of technically pure nitrogen with oxygen impurities for nitriding. However, this amount of oxygen was not enough for the formation of an oxynitride layer. This was also confirmed by X-ray analysis of the phases in the nitrided layer, which confirmed the presence of only titanium compounds with nitrogen such as Ti2N and TiNx (Fig. 3).

**Table 1.** Elemental composition of surface layers of VT6 titanium alloy after different types of TCT

| Element | Oxidation | | Nitriding | |
|---|---|---|---|---|
| | Wt.% | At.% | Wt.% | At.% |
| N | 0.00 | 0.00 | 9.45 | 20.52 |
| O | 14.28 | 30.48 | 4.28 | 9.54 |
| Al | 4.51 | 5.67 | 4.49 | 5.88 |
| V | 3.02 | 2.08 | 3.91 | 2.72 |
| Ni | 0.12 | 0.08 | 0.13 | 0.10 |
| Fe | 0.30 | 0.17 | 0.18 | 0.11 |
| Ti | balance | | balance | |

Since the atomic radius, solubility and diffusion mobility of oxygen and nitrogen in titanium differ significantly, the surface layers formed on the surface of the analyzed alloy differed in strength (depending on the temperature-time conditions of saturation and control of the oxygen or nitrogen content in the composition of the media during TCT). In particular, the microhardness $HV_{0.49}$ on the surface of titanium after its solid solution hardening in an oxygen-containing environment was more than twice as high as that characteristic of titanium in the initial state (7.3 and 3.6 GPa, respectively). And this despite the fact that the titanium oxide film on its surface was not visualized at all. The increased hardness of the oxidized layer was felt at a depth of up to ~30 μm. Nitriding caused the appearance of two layers on the surface of titanium. In the upper one with a thickness of up to 3 μm, titanium nitrides ($TiN_x$+$Ti_2N$) were formed, and only under this layer was a sublayer formed based on a solid solution of nitrogen in α-titanium with a thickness of ~ 20 μm. As a result, the surface microhardness of nitrided titanium increased almost threefold (up to 9.4 GPa). Common to both variants of TCT was the disappearance of the positive effect of solid-solution hardening of titanium on its microhardness with deepening into the hardened layers. It was believed that this was caused by the different content of the elements of the embodiment at different depths of their diffusion penetration. After all, at a temperature of 750°C, the diffusion coefficient of nitrogen in α-titanium is 6...7 times smaller than that of oxygen. In particular, the diffusion coefficient of oxygen in α-titanium calculated according to the Arrhenius equation was $\sim 2.62\times10^{-15}$, and that of nitrogen was $\sim 3.14\times10^{-16}$ $m^2/s$. As a result, oxygen was able to penetrate to a greater depth into the cross-section of the titanium sample, which resulted in a greater thickness of the hardened layer during oxidation compared to nitriding. A feature of the use of oxidation and nitriding was also a significant (more than 4.5 times) increase in the surface roughness Ra of the VT6 alloy after TCT (from 0.065 to 0.23 μm). Moreover, the effect on the Ra index did not depend on the environment used for TCT.

### 3.2. Morphological Features of Wear Tracks

Analysis of the wear track profiles on both types of solid-solution-hardened layers revealed distinct deviations from the behavior of untreated titanium. While the untreated VT6 alloy typically exhibits a traditional wear groove geometry (Fig. 1b), the oxidized and nitrided specimens showed irregular profiles with non-uniform depth distributions (Fig. 4).

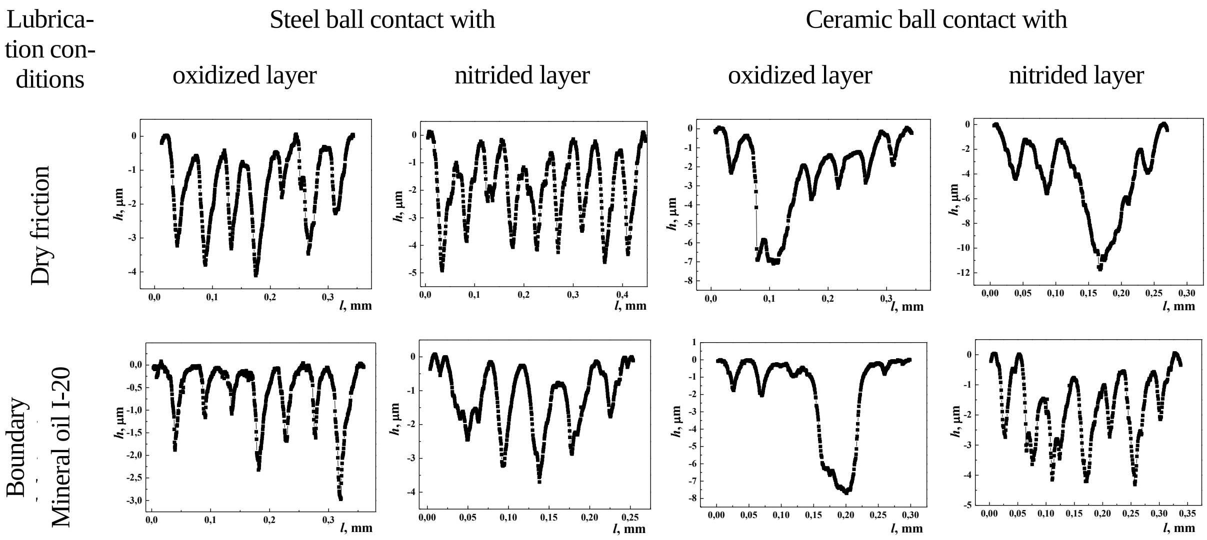

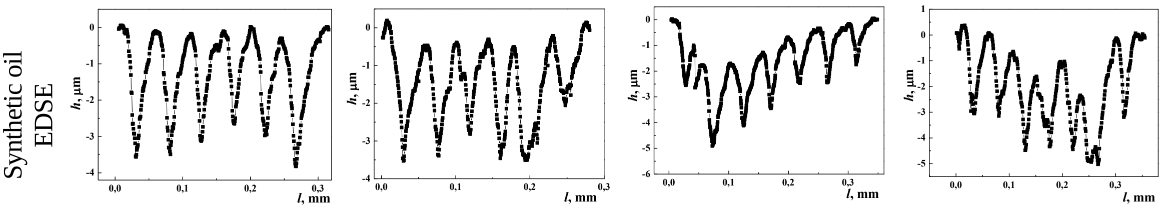


**Figure 4.** Representative cross-sectional profiles of wear tracks on oxidized and nitrided VT6 alloy surfaces following oscillatory sliding against steel and ceramic counterbodies under dry friction and boundary lubrication (mineral I-20 or synthetic EDGE oils).

These variations in wear track morphology are attributed to the interaction between the hardened sublayers and significantly harder second-phase particles ($TiO_2$ or TiN). Although the microhardness of the diffusion zones decreases from 7.3–9.4 GPa at the surface to the base level of 3.6 GPa at depths of 20–30 μm, the presence of extremely hard surface phases (8 GPa for $TiO_2$ and up to 24 GPa for TiN) fundamentally alters the wear mechanism. Due to their high hardness, these oxide and nitride particles become embedded into the surface of either the steel or ceramic counterfaces, acting as micro-cutters that produce deep scratches (plowing) on the specimen surface under all lubrication conditions. The density of these depressions was highest during dry sliding against the steel ball, slightly lower against the ceramic ball, and reached a minimum under lubricated conditions. This suggests that wear during oscillating friction occurs through the stepwise removal of thin chips by these hard particles. In dry friction tests against a steel ball, the maximum depth of the wear tracks on both types of coatings did not exceed 4–5 μm. Under boundary lubrication, this depth decreased to 3.0–3.5 μm. This reduction is attributed to the flushing effect of the lubricant, which removes hard wear debris from the contact zone and prevents its embedding into the counterface, thereby mitigating the micro-cutting process.

Frictional interaction with the ceramic ball resulted in wear track profiles that maintained the previously observed irregular relief (Fig. 4). However, the maximum depth of these depressions generally increased compared to those formed against the steel counterface. Furthermore, the ceramic counterface produced a more pronounced wear groove, a feature that was nearly absent in tests with the steel ball. This behavior is attributed to the superior hardness of the ceramic material, which inhibits the embedding of hard $TiO_2$ or TiN particles into its surface. Consequently, the intrinsic hardness of the ceramic ball becomes the dominant factor, leading to more intensive abrasive wear of the hardened titanium layers. The comparable depths of the depressions on both oxidized and nitrided layers when lubricated with EDGE synthetic oil further support this; as wear debris is partially flushed from the contact zone, the influence of the counterface material properties becomes more significant than the specific type of TCT.

The complex geometry of the wear track cross-sections necessitated a refined methodological approach for calculating the wear area. Conventional quantitative estimates, which rely on simple geometric averaging, were replaced by a sectional integration method. The total cross-sectional area was determined by partitioning the profile into individual segments corresponding to each depression. The area of each segment was calculated based on its specific geometry, and these values were summed to determine the total cross-sectional area for a given section. By integrating these areas over the total sliding path, the total wear volume was precisely quantified, characterizing the material loss of the surface-hardened layers.

### 3.3. Tribological Performance and Wear Resistance

The wear resistance of the oxidized VT6 alloy surface was consistently higher than that of the nitrided surface, regardless of the counterface material or lubrication conditions (Table 2). This phenomenon is attributed to the higher intrinsic hardness of the nitrided layer (Table 1).

**Table 2.** Wear volume* (V × 103 μm3) of oxidized and nitrided VT6 alloy surface layers under oscillating friction against steel and ceramic counterbodies

| Lubrication conditions during friction | Steel ball contact with | | Ceramic ball contact with | |
|---|---|---|---|---|
| | oxidized layer | nitrided layer | oxidized layer | nitrided layer |
| No lubrication | 0.52 | 0.82 | 0.77 | 1.13 |
| Mineral oil I-20 | 0.26 | 0.41 | 0.52 | 0.57 |
| Synthetic oil EDSE | 0.24 | 0.33 | 0.56 | 0.70 |

*In this case, the value of wear of the reinforced layer due to friction was estimated by volumetric losses determined by multiplying the average value of the cross-sectional area of the wear groove by its length.

During the friction process, extremely hard (24 GPa) TiN micro-particles are generated as wear debris. These particles act as an abrasive medium, scratching both the specimen surface and the counterface. The resulting increase in counterface roughness further accelerates the wear of the nitrided layer. In contrast, $TiO_2$ particles from the oxidized layer, possessing a lower hardness (7–8 GPa), exhibit a less aggressive abrasive effect on the counterfaces, thereby preserving the integrity of the surface-hardened layer for a longer duration. The introduction of lubrication into the contact zone between the steel ball (8 GPa) and the hardened layers reduced wear by more than 50% (Table 2). While the oxidized layer showed no significant sensitivity to the lubricant type, the nitrided layer exhibited 25% higher wear resistance in synthetic oil compared to mineral oil.

A significant increase in wear was observed when the steel ball was replaced with a ceramic counterface (20 GPa). Under dry friction, wear increased by up to 40%. Paradoxically, under boundary lubrication, the wear rate approximately doubled compared to the values recorded with the steel counterface. This unexpected result contradicts the conventional assumption that lubricants primarily reduce wear by flushing debris from the contact zone. The intensification of wear in the presence of lubricants when using a ceramic counterface suggests that additional, yet unidentified, factors-possibly related to the chemical interaction or the specific rheology of the debris-oil mixture-influence the tribological behavior of solid-solution-hardened titanium alloys.

### 3.4. Evolution of Friction Coefficients

Under dry sliding conditions, the friction coefficient (f) of the oxidized VT6 alloy layers exhibited an upward trend for both types of counterfaces, with this effect being most pronounced when paired with the ceramic ball (Fig. 5).

Specifically, while $f$ increased from 0.12 to 0.14 against the steel ball, it reached 0.3 when tested against the ceramic ball. A similar, yet more intense, increase in $f$ was observed for the nitrided layer in contact with the ceramic counterface. In contrast, during tests with the steel ball, the friction coefficient of the nitrided layer remained stable throughout the duration of the test, albeit at a higher baseline ($f \approx 0.2$) compared to the oxidized layer.

The introduction of lubrication (either mineral or synthetic oil) into the contact zone effectively stabilized the friction coefficient for both the oxidized and nitrided layers. In all lubricated tests, $f$ remained constant within the range of 0.12–0.14 for the entire test period (Fig. 5). This stability serves as direct evidence of the lubricant's efficiency in flushing wear debris from the contact interface. Consequently, under boundary lubrication, the choice of lubricant effectively stabilizes the frictional behavior and, by extension, the wear rate of TCT-hardened VT6 alloy.

Notably, in dry friction against a ceramic ball, the $TiO_2$ coating showed a significant tendency toward an increasing friction coefficient. However, the addition of oil regardless of its type (mineral or synthetic) mitigated this effect, ensuring a stable friction coefficient not exceeding $f = 0.14$ for all investigated surface modifications.

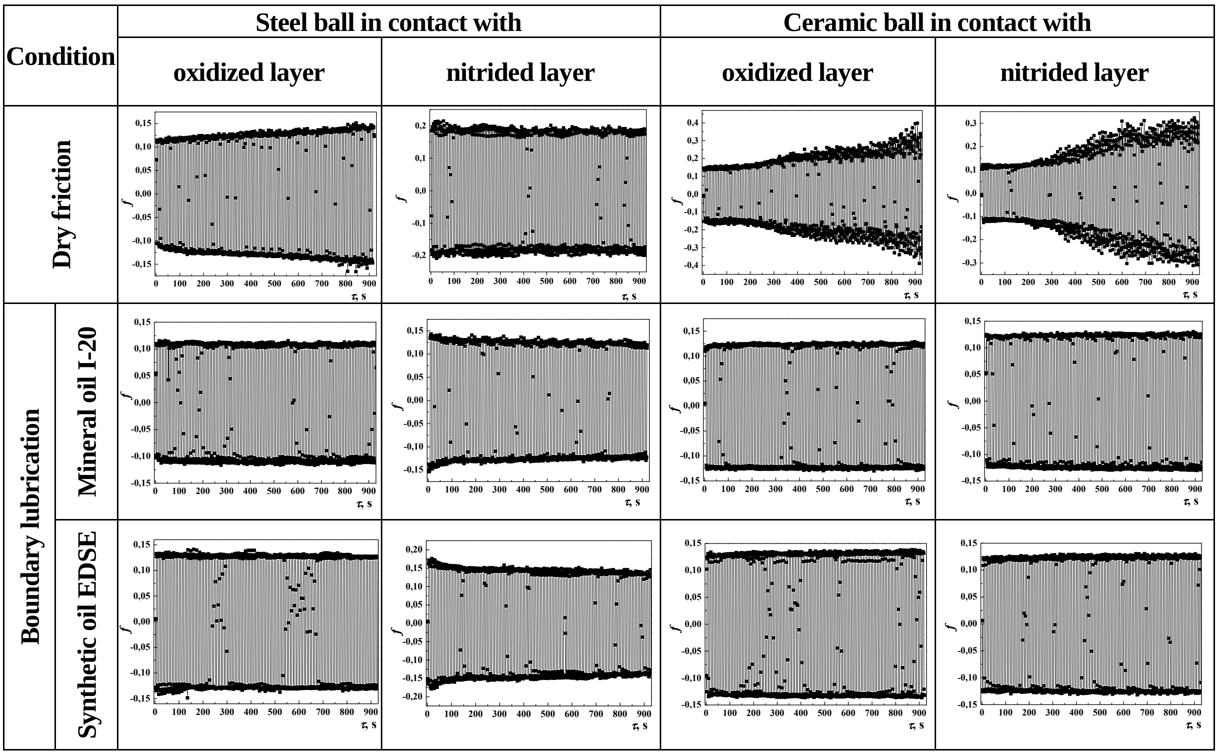


**Figure 5.** Evolution of the friction coefficient for oxidized and nitrided VT6 alloy specimens during friction tests by oscillatory sliding against steel and ceramic counterfaces. Results are shown for dry friction and boundary lubrication conditions using mineral (I-20) and synthetic (EDGE) oils.

## 4. CONCLUSIONS

Thermochemical treatment (TCT) of the VT6 titanium alloy in controlled oxygen or nitrogen environments significantly enhanced surface microhardness, increasing it from the base value of 3.6 GPa (345 $HV_{0.49}$) to 7.3 GPa (744 $HV_{0.49}$) for oxidized layers and 9.4 GPa (939 $HV_{0.49}$) for nitrided layers.

Wear track cross-sections on oxidized and nitrided surfaces showed irregular patterns with deep, localized depressions. This morphology of the friction surface is attributed to the embedding of hard titanium dioxide or nitride particles into the counterbody (steel or ceramic balls). During friction they act as micro-cutters, intensifying surface wear through a plowing mechanism and the removal of fine chips. As a result, small scratches appear on the friction surface, and a significant difference in the relief of the wear track profile is observed across its entire width.

Under oscillatory sliding friction, the oxidized VT6 alloy demonstrated 40–50% higher wear resistance compared to the nitrided layer. This trend was consistent across all counterface materials, lubrication states, and lubricant types (mineral I-20 or synthetic EDGE oil). At higher hardness, nitrided layers on the VT6 alloy demonstrated lower wear resistance than oxidized layers. This is explained by the abrasive action of TiN wear debris, which increases counterface roughness and accelerates material removal from the hardened layers on the titanium alloy.

During dry friction tests against a steel ball, the friction coefficient remained stable for both modified layers. However, when paired with a ceramic ball, the friction coefficient began to increase after 200–300 s of testing. This behavior is associated with the dominant role of the ceramic counterface hardness in the friction process as the contact evolves.

In boundary lubrication conditions, the friction coefficient for all tested pairs remained stable throughout the testing period. This stability is attributed to the effective flushing of hard wear products ($TiO_2$ or TiN particles) from the contact zone by the lubricant, preventing their abrasive interaction with the surface.

**Author Contributions:** Conceptualization: M. Student, I. Pohrelyuk; Methodology: Kh. Zadorozhna, O. Student, V. Trush, V. Hvozdetskyi; Validation: Kh. Zadorozhna, V. Trush, V. Hvozdetskyi; Formal analysis: M. Student, A. Luk'yanenko; Writing – original draft preparation: M. Student, A. Luk'yanenko; Writing – review and editing: A. Luk'yanenko, O. Student; Supervision: I. Pohrelyuk.

**Funding:** This work was supported by the National Research Foundation of Ukraine within the framework of project No. 2025.06/0028: «Development of technology for surface strengthening of titanium alloy parts of aircraft engines by regulated diffusion saturation with interstitial elements».

**Conflicts of Interest:** The authors declare no conflict of interest.

**Data Availability Statement:** Data included in the article: All data generated or analyzed during this study are included in this published article.

**Declaration of Generative AI and AI-assisted technologies in the writing process:** During the preparation of this work, the authors used Google Gemini in order to improve the English language (grammar and style). After using this service, the authors reviewed and edited the content as needed and takes full responsibility for the content of the publication.

## REFERENCES

[1] Leokha F. L., Khrychikov V. E. (2025) Current trends in the production and application of titanium alloys. Theory and Practice of Metallurgy, 4, pp. 30 36. https://doi.org/10.15802/tpm.4.2025.05.

[2] Titanium and Titanium Alloys. Fundamentals and Applications. Edited by Christoph Leyens, Manfred Peters. WILEY-VCH Verlag GmbH & Co. KGaA, Weinheim. 2003. 514 p. ISBN: 3-527-30534-3.

[3] Titanium-Based Alloys – Characteristics and Applications. Edited by Petrica Vizureanu and Madalina Simona Baltatu. London, IntechOpen, United Kingdom. 2024. 190 p. http://dx.doi.org/10.5772/intechopen.1001617.

[4] Iasnii V., Yasniy O., Homon S., Budz V., Yasniy P. (2023) Capabilities of self-centering damping device based on pseudoelastic NiTi wires. Engineering Structures, 278, 115556. http://dx.doi.org/10.1016/j.engstruct.2022.115556.

[5] Iasnii V., Bykiv N., O. Yasniy, V. Budz (2022) Methodology and some results of studying the influence of frequency on functional properties of pseudoelastic SMA. Scientific journal of the Ternopil national technical university, 107, pp. 45–50. http://dx.doi.org/10.33108/visnyk_tntu2022.03.045.

[6] Iasnii V. (2020) Main regularities of influence of cyclic loading parameters on the module of elasticity austenite of shape memory alloys. Herald of Khmelnytskyi national university, 289, pp. 131–135. https://www.doi.org/10.31891/2307-5732-2020-289-5-131-135.

[7] Williams J. C., Boyer R. R. (2020) Opportunities and Issues in the Application of Titanium Alloys for Aerospace Components. Metals, 10 705. https://www.doi.org/10.3390/met10060705.

[8] Chen Y., Zhang H., Wang B., Huang J., Zhou M., Wang L., Xi Y., Jia H., Xu S., Liu H., Wen L., X. Xiao, Liu R., Ji J. (2024) A Review of Research on Improving Wear Resistance of Titanium Alloys. Coatings, 14, 786. https://doi.org/10.3390/coatings14070786.

[9] Kandrotaitė J. R., Blažys G., Mažeika D., Syzonenko O. D. (2024) Tribological investigation of titanium composite materials used in aviation. International Scientific Journal "Machines. Technologies. Materials", XVIII, 5, pp. 171–175.

[10] Rundora N. R., Klenam D. E. P., Polat S., Mathabathe N. M., J.s van der Merwe, Bodunrin M. O. (2024) Dry Sliding Wear Behavior of Experimental Low-Cost Titanium Alloys. Tribology Transactions, 67, pp. 560–572. https://doi.org/10.1080/10402004.2024.2357288.

[11] Yang C.-H., Li C.-Y., Chan C.-C., Chi P.-C., Shih J.-H., Liao F.-Y., Chang S.-H. (2025) Effect of Low-Pressure Gas Oxynitriding on the Microstructural Evolution andWear Resistance of Ti-6Al-4V Alloy. Lubricants, 13, 449. https://doi.org/10.3390/lubricants13100449.

[12] Meng Y., Villa M., Dahl K. V., Wang B., Drouet M., Dubois J.-B., Somers M. A. J., Christiansen T. L., (2021) Thermochemical surface hardening of Ti-6Al-4V: On the role of temperature and treatment media. Surface and Coatings Technology, 422, 127505. https://doi.org/10.1016/j.surfcoat.2021.127505.

[13] Dziri A., Ammar K., Forest S., Proudhon H., Sirvin Q., T. Richeton D. Texier, Effect of oxygen content on elastic properties of an oxygen-graded titanium: Experimental and computational analyses, Materials & Design. 259 (2025) 114801. https://doi.org/10.1016/j.matdes.2025.114801.

[14] Li W., Ma Z., Yang Z., Wang S. (2025) Effect of high-temperature oxidation on mechanical properties of TC11 titanium alloy. Journal of Materials Research and Technology, 36, ppю 3634–3646. https://doi.org/10.1016/j.jmrt.2025.04.071.

[15] Pohrelyuk I. M., Student M. M., Zadorozhna Kh. R., Lavrys S. M., Kravchyshyn T. M., Kovalchuk I. V. (2024) Tribological Characteristics of Titanium after Combined Treatment. Materials Science, 59, pp. 746–753. https://doi.org/10.1007/s11003-024-00836-0.

[16] Li W., Wang S., Yang X., Duan H., Wang Y., Yang Z., (2025) Research Progress on Fatigue Damage and Surface Strengthening Technology of Titanium Alloys for Aerospace Applications, Metals, 15, 192. https://doi.org/10.3390/met15020192.

[17] Tkachuk O. V., Hvozdetskyi V. M., Student M. M., Zadorozhna Kh. R., Kovalchuk I. V., Pohrelyuk I. M. (2025) Structural features and wear resistance of the TiAlN coating formed on the Ti–6Al–4V alloy by combining electric arc spraying and gas nitriding methods. Materials Science, 60, pp. 577–583. https://doi.org/10.1007/s11003-025-00905-y.

[18] Binti A. B. M., Pinke P., Tóth L., Kovács T. A. (2024) Heat-treating processes of the titanium alloys. Műszaki Tudományos Közlemények, 21, pp. 56–60. https://doi.org/10.33894/mtk-2024.21.08.

[19] Student M. M., Pohrelyuk I. M., Luk'yanenko A. G., Student O. Z., Zadorozhna Kh. R., Hvozdetsky V. M. (2025) Improving the tribological characteristics of the surface layers of titanium alloy VT6 by diffusion saturation with interstitial elements, Phys.-Chem. Mechanics of Materials, 61, pp. 57–64. https://doi.org/10.15407/pcmm2025.06.057 (In Ukrainian).